ELSEVIER

International Journal of Fatigue 23 (2001) 375–382

International Journal of Fatigue

www.elsevier.com/locate/ijfatigue

Fatigue crack propagation in aluminium alloy foams

O.B. Olurin, K.Y.G. McCullough, N.A. Fleck *, M.F. Ashby

University of Cambridge, Department of Engineering, Trumpington Street, Cambridge CB2 1PZ, UK

Received 17 July 2000; accepted 15 January 2001

Abstract

The mode I fatigue crack propagation (FCP) response of the closed-cell aluminium alloy foams Alulight and Alporas have been measured for a relative density in the range 0.1 to 0.4. The validity of linear elastic fracture mechanics (LEFM) to characterise the fatigue crack propagation (FCP) response is demonstrated, and *K*-increasing and *K*-decreasing tests are used to determine the full shape of the FCP response. The classical sigmoidal variation of log d*a*/d*N* with log ΔK is evident, with a Paris-law exponent m=20 for Alulight and m=25 for Alporas. The effects of relative density, mean stress and a single peak overload on the FCP response are investigated. The study concludes by analysing the mechanism of fatigue crack growth; it is suggested that the fatigue crack growth rate is controlled by the progressive degradation of crack bridging by fatigue failure of the cell edges behind the crack tip.

Keywords: Aluminium foams; Fatigue crack propagation; Small-scale bridging

1. Introduction

Recent developments in manufacturing methods [1–5] have given rise to a range of commercially viable metallic foams. Two of these — Alulight[1] and Alporas[2] — are the subject of the present study. Alulight is produced by a powder metallurgy route, and is available in cylinders or panels with a relative density ranging from 0.1 to 0.4, and in a wide range of compositions, including the Al–Si casting range of alloys. Alporas is commercially available in plate form, of composition Al–Ca1.5–Ti1.5 (wt%), and with a relative density in the range 0.08 to 0.15. It is manufactured by a batch casting process; like Alulight, the foaming process is by thermal decomposition of titanium hydride, with the titanium remaining in solution.

The successful implementation of metallic foams for structural applications, such as the cores of sandwich panels, is dependent upon an understanding of their mechanical properties including their resistance to fatigue crack growth. Recent tests [6–8] to measure the stress–life fatigue behaviour of uncracked metallic foams have shown that the Alulight and Alporas closed-cell aluminium-based foams have promising fatigue properties, with about the same ratio of cyclic strength to monotonic strength as that of solid aluminium alloys.

Fatigue crack growth, by contrast, is unexplored: the dependence of crack growth rate d*a*/d*N* upon the stress intensity range ΔK is not known. In the present study, the validity of using linear elastic fracture mechanics (LEFM) to characterise the applied fatigue loading is demonstrated and *K*-increasing and *K*-decreasing tests are used to determine the fatigue crack propagation (FCP) response. The FCP threshold ΔK_{th} is measured and the effects of relative density, mean applied stress and a single peak overload on the FCP response are evaluated. The extent of a crack bridging zone and the micromechanism of crack growth are also determined.

2. Material specification and experimental procedure

Rectangular plates of Alulight Al–Mg1–Si0.6 and Al–Mg1–Si10 foams were manufactured to the dimensions 145 mm by 145 mm by 9 mm, with a fully dense skin

* Corresponding author. Tel.: +44-1223-332650; fax: +44-1223-765046.

E-mail address: nafl@eng.cam.ac.uk (N.A. Fleck).

[1] Supplier: Mepura Metallpulvergesellschaft mbH, Ranshofen, A-5282 Braunau–Ranshofen, Austria.

[2] Supplier: Shinko Wire Company Ltd, 10-1, Nakahama-machi, Amagasaki-shi, 660 Japan.

0142-1123/01/$ - see front matter
PII: S0142-1123(01)00010-X

of thickness of the order of 1–2 mm. Since the primary focus of this study is the effect of foam density and composition upon the FCP response, the skins were removed by wire electro-discharge machining, giving a net specimen thickness B of 7.5 mm (approximately 10 cells). The Alporas foam was obtained from the material supplier in blocks of dimensions 0.5 m×0.5m×50 mm; each block was of uniform density and was electro-discharge machined to a thickness of 25 mm.

Compact tension (CT) specimens of width W=50 mm for the Alulight specimens and width W=100 mm for the Alporas specimens were electro-discharge machined from the as-received blocks. The relative density $\bar{\rho}$ of the as-machined specimens was $\bar{\rho}$=0.1 to 0.4 for Alulight and $\bar{\rho}$=0.08 to 0.15 for Alporas. (The precise value of $\bar{\rho}$ for each specimen was obtained by weighing to an accuracy of four significant figures.) The *mean* cell size l of Alulight foams varies with relative density according to the relation [9,10]

$$l \approx l_0(1-2.22\bar{\rho}), \tag{1}$$

where l_0=2.25 mm. For example, l≈1.5 mm for a foam of relative density $\bar{\rho}$=0.15, whereas l≈0.5 mm for a foam of relative density $\bar{\rho}$=0.35. For Alporas, the average cell size equals 3.5 mm for all densities.

The compact tension specimens were reinforced in the vicinity of the loading holes by Tufnol facings of thickness 3 mm for Alulight and 5 mm for Alporas to prevent pull-out of the loading pins. The fatigue tests were performed at room temperature using a servo-hydraulic test machine in sinusoidal load control at a frequency of 20 Hz, from an initial notch length of a_0/W=0.3 and root radius of 0.05 mm. We note in passing that preliminary tests confirmed that the fatigue crack propagation response was independent of the loading frequency over the range 0.1–50 Hz. We shall argue below that ΔK can be used to characterise the fatigue loading of the Alulight and Alporas foams specimens. The K-calibration for the CT geometry as given by ASTM E647-95 [11] was employed. On writing the maximum and minimum loads in each fatigue cycle as P_{max} and P_{min}, respectively, the load ratio R is defined by $R=P_{min}/P_{max}$.

An evaluation of the FCP response relies upon an accurate measurement of crack growth. Visual observations using a travelling microscope revealed the presence of a single dominant fatigue crack, with intermittent bridging along its wake. The direct current (DC) potential drop method was used to monitor crack extension since, for fully dense metals, it can determine crack growth to an accuracy of about 0.01 mm [12]. The apparatus adopted here is illustrated in Fig. 1. Additional experimental details are given in Ref. [10]. Crack length measurements from a travelling microscope and from the back-face compliance technique [13] were used to check the accuracy of the potential drop readings. The measured crack length by potential drop, back-face compliance and visual observation were all in good agreement, such that the deduced crack growth rate da/dN at a given ΔK level agreed to within 10% for the three methods. The potential drop method was used as the primary method for logging crack length versus cycles. The crack growth rate da/dN was calculated by a moving quadratic fit to the a–N data, in accordance with the standard ASTM E647-95 [11].

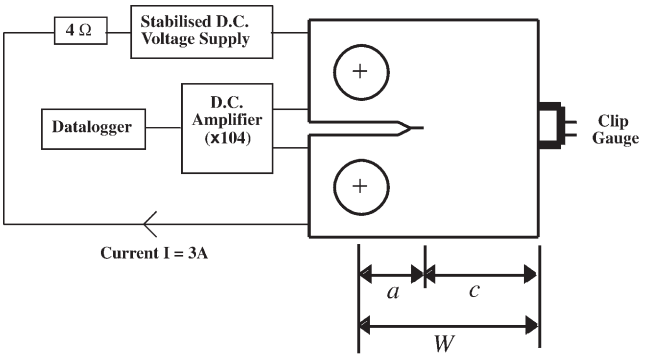

Fig. 1. Test apparatus.

3. Validity of using K to characterise the applied fatigue loading

Recent studies on the fracture toughness of Alulight [10] and Alporas [14] made use of compact tension specimens of width W=50 mm and 100 mm; in these tests a zone of crack bridging developed over about four cell dimensions from the notch root to the growing crack tip, with full plastic collapse across the uncracked ligament. Consequently, the conditions of small-scale bridging (SSB) and small-scale yielding (SSY) do not apply, and the conditions at the crack tip cannot be characterised simply in terms of the applied stress intensity K. In contrast, we shall show for similar specimens subjected to fatigue loading that both SSY and SSB assumptions hold, and ΔK can be used to characterise the fatigue response.

3.1. Validity of small-scale yielding

Conformity with the small-scale yielding assumption is usually ensured by checking that both the uncracked ligament $(W-a)$ and the crack length a of a compact tension specimen satisfy

$$(W-a, a) \geq 2.5\left(\frac{\Delta K}{2\sigma_{pl}}\right)^2, \tag{2}$$

where ΔK is the stress intensity range of the fatigue cycle and σ_{pl} is the (tensile) monotonic yield strength of the specimen. This is an extension of the usual specimen size criterion in a fracture toughness test, with the role

of K_{max} replaced by ΔK and the monotonic yield strength σ_{pl} replaced by $2\sigma_{pl}$ in order to estimate the cyclic plastic zone size [15]. This criterion was satisfied for both materials in all fatigue tests. Since the cyclic plastic zone is of magnitude $(1/\pi)(\Delta K/2\sigma_{pl})^2$, we conclude that the cyclic plastic zone is much less than the leading specimen dimensions, and so small-scale yielding conditions pertain.

3.2. Validity of small-scale bridging

The extent of crack bridging in the wake of a growing fatigue crack was determined by direct visual observation of the fatigue crack. A scanning electron micrograph of the side face of an Alulight specimen is shown in Fig. 2, with the position of the crack tip indicated. A small bridging zone (of dimension one cell) exists behind the crack tip, such that the cell faces have cracked but the cell edges have not. (This is consistent with the notion that the cell faces undergo membrane tension, whereas the cell edges deform in bending [6].) A similar examination of cracked Alporas specimens also revealed a bridging zone of length about one cell size.

Additional support for the magnitude of the bridging zone was obtained by interrupting several tests and by removing the crack wake using a jeweller's saw. Potential drop and back-face compliance measurements revealed that the apparent crack length only began to increase when the saw had advanced to within one cell dimension behind the optically observed crack tip, indicating complete crack face separation except over the short bridging zone. It is concluded that small-scale bridging (SSB) conditions prevail in fatigue crack growth for both foams.

4. Results

4.1. Typical da/dN versus ΔK response

In line with the recommendations of ASTM E647-95 [11], three forms of fatigue test were performed:

1. *K*-increasing tests, used to measure crack growth rates $da/dN > 10^{-5}$ mm/cycle. In these tests, performed at a constant load amplitude (constant ΔP), ΔK was allowed to increase as the crack length increases.
2. *K*-decreasing tests, used to measure crack growth rates $da/dN < 10^{-5}$ mm/cycle. These tests were performed at a constant normalised *K*-gradient $c=(1/K)(dK/da)=-0.08$ mm^{-1} by manual load shedding at crack growth intervals of $\Delta a=0.5$ mm, in accordance with ASTM E647-95 [11]. Loads were shed until no crack growth (i.e., less than 0.01 mm) was detected over 10^7 cycles.
3. *K*-constant tests, used to investigate bridging of the crack wake and the effect of a single peak overload on the FCP response. The details are the same as for the *K*-decreasing tests, but with $c=0$.

Fig. 3 shows typical fatigue crack propagation results for specimens of relative density $\bar{\rho}=0.19$, tested at the load ratio $R=0.1$. It is clear from this figure that the crack growth rate da/dN is a unique function of ΔK, and independent of whether *K* is increasing, decreasing or constant during the tests. The classic sigmoidal variation of $\log da/dN$ with $\log \Delta K$ is evident, with a Paris-law exponent $m \approx 20$.

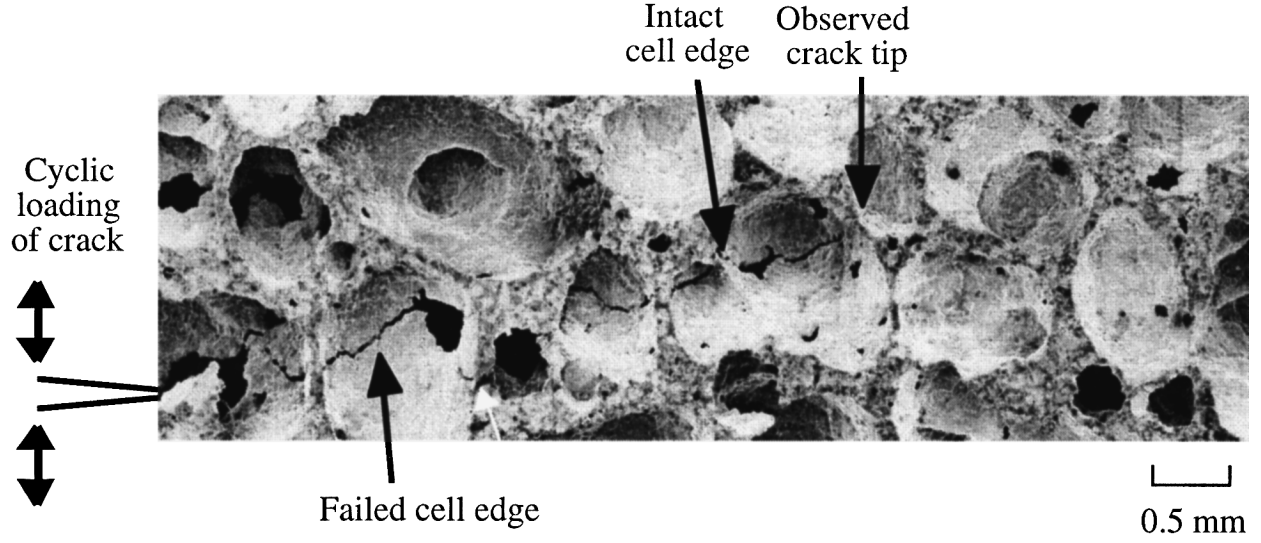

Fig. 2. Scanning electron micrograph of a cracked compact tension specimen of Alulight foam, of composition Al–Mg1–Si0.6 with $\bar{\rho}=0.29$. The crack has grown $\Delta a=8$ mm at 10^{-5} mm/cycle, by applying a constant $\Delta K=1.12$ MPa m$^{1/2}$ with $R=0.1$.

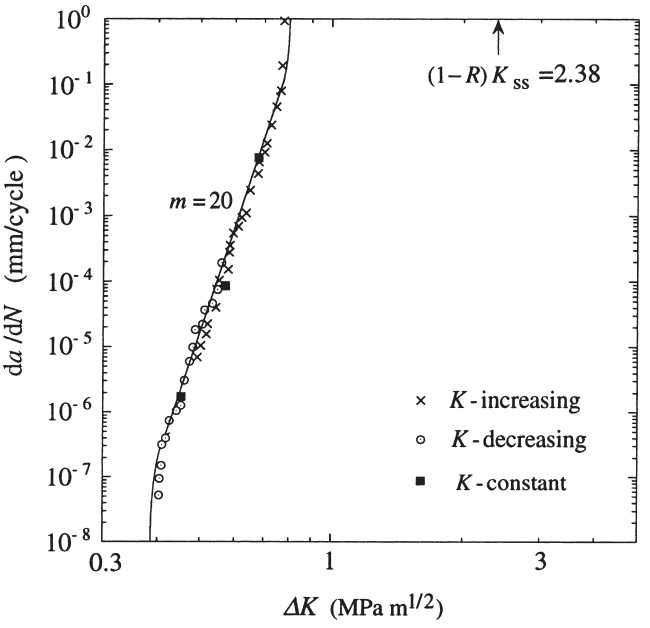

Fig. 3. Comparison of da/dN from K-increasing, K-decreasing and K-constant tests. Tests were performed at R=0.1 on compact tension specimens of Alulight foam, of composition Al–Mg1–Si0.6 with $\bar{\rho}$=0.19.

4.2. Determination of the fatigue crack propagation threshold, ΔK_{th}

From Fig. 3, the relationship between log da/dN and log ΔK becomes non-linear for an average crack growth increment of less than about 5×10^{-7} mm/cycle. The standard ASTM E647-95 [11] suggests an arbitrary operational definition of the threshold stress intensity range ΔK_{th} as that value of ΔK which corresponds to da/dN=1×10^{-8} mm/cycle. However, FCP rates below da/dN=5×10^{-8} mm/cycle were not achieved with Alulight: when ΔK was reduced to investigate these rates, no crack growth was evident for 10^7 cycles to within the resolution of the crack extension measurements (0.01 mm). In such cases, the ΔK at which no crack growth occurred can be defined as ΔK_{th} (see, for example, Suresh [15]). For the results shown in Fig. 3 this corresponds to a threshold value of ΔK_{th}=0.40 MPa m$^{1/2}$. However, given the sensitivity of da/dN to ΔK and the scatter in growth rates exhibited by apparently identical specimens, a more conservative value for ΔK_{th} might be considered appropriate for design purposes. A simple conservative estimate can be attained by extrapolating the linear regime of the Paris curve down to da/dN=10^{-8} mm/cycle and taking the corresponding ΔK to be ΔK_{th}. This method has the added benefit of allowing an operational definition of ΔK_{th} from a (time-saving) K-increasing test. For the results shown in Fig. 3, the extrapolation method implies ΔK_{th}=0.34 MPa m$^{1/2}$, which is only 15% less than the measured value of 0.40 MPa m$^{1/2}$.

4.3. Effect of silicon content of Alulight on the fatigue crack propagation response

In order to investigate the effect of silicon content of Alulight upon the da/dN versus ΔK response, K-increasing tests were performed on compact tension specimens of the Al–Mg1–Si0.6 and the Al–Mg1–Si10 foams. Fig. 4 shows typical results, plotted on double log axes, from specimens of relative density $\bar{\rho}$=0.23 tested at R=0.1. For both compositions of foam, the observed slope was $m\approx20$; however, Al–Mg1–Si10 has a lower fatigue resistance than the Al–Mg1–Si0.6 foam, consistent with its lower fracture toughness [10].

4.4. Effect of relative density $\bar{\rho}$ on the fatigue crack propagation response

The effect of relative density upon the da/dN versus ΔK response is shown in Fig. 5(a) for Al–Mg1–Si0.6 Alulight and in Fig. 5(b) for Alporas, at R=0.1. For each of the densities studied, the shape of the da/dN versus ΔK response is qualitatively similar to that shown in Fig. 3, with a Paris-law exponent $m\approx20$ for Alulight and $m\approx25$ for Alporas. As expected, for a given crack growth rate, the stress intensity range ΔK increases with increasing $\bar{\rho}$, see Fig. 5. In Fig. 6, the ΔK corresponding to da/dN=10^{-4} mm/cycle is cross-plotted against $\bar{\rho}$ using log–log axes. Power-law fits with an exponent of 1.71 for Alulight and 1.60 for Alporas adequately describe the responses. In similar fashion, the steady-state fracture toughness K_{ss} in monotonic fracture tests scales with $\bar{\rho}^{1.75}$ for both Alulight and Alporas [10,14]. (We

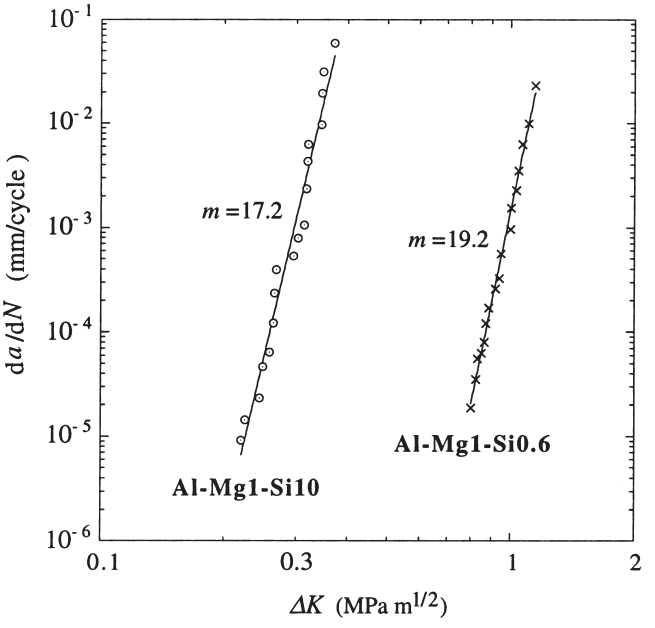

Fig. 4. Effect of silicon content on the da/dN versus ΔK response. K-increasing tests at R=0.1 on compact tension specimens of Alulight foam with $\bar{\rho}$=0.23.

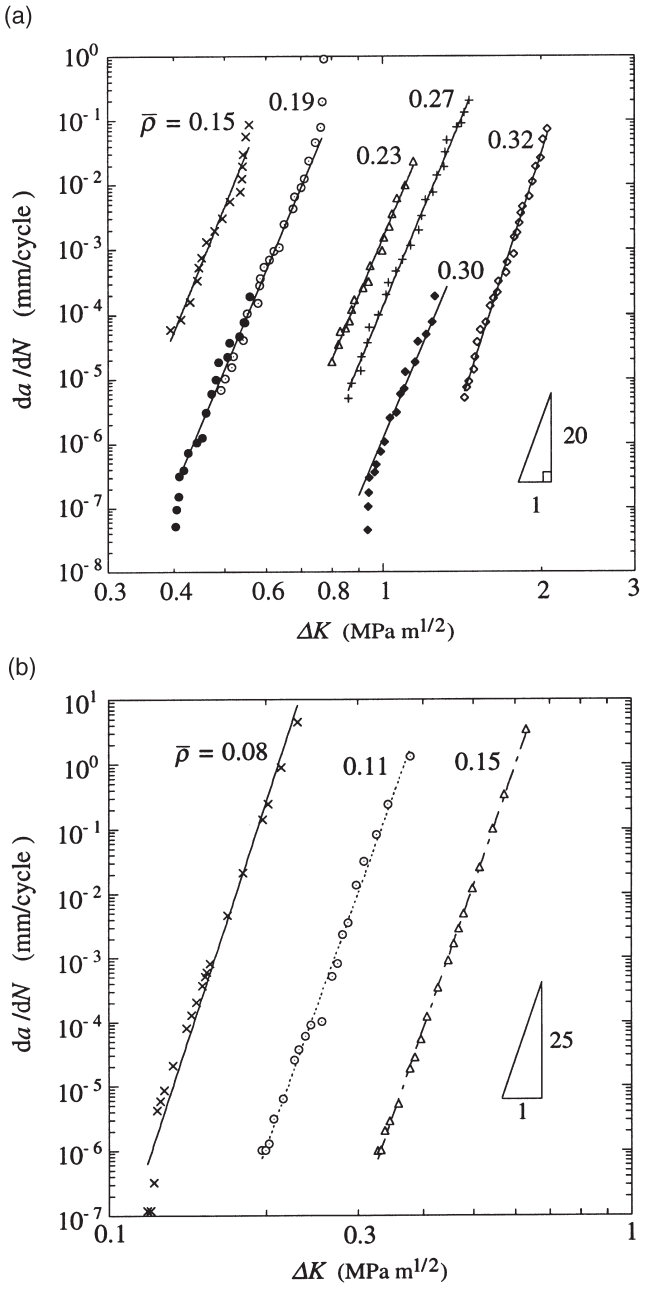

Fig. 5. Effect of relative density $\bar{\rho}$ on the da/dN versus ΔK response at R=0.1 for (a) Alulight foam and (b) Alporas foam. The data for Alulight of relative density $\bar{\rho}$=0.19 are obtained from K-decreasing tests at low growth rates, and from K-increasing tests at high growth rates.

remind the reader that K_{ss} is the asymptotic, steady-state value of fracture toughness after substantial crack growth in a monotonic toughness test.)

In Fig. 7, the crack growth rate data of Fig. 5 are re-plotted against $\Delta K/\bar{\rho}^{1.71}$ for Alulight and against $\Delta K/\bar{\rho}^{1.60}$ for Alporas, using log–log axes. For each foam, the data collapse on to a single curve, to within material scatter. In the Paris regime of the graph, the following power-law fit adequately summarises the FCP response

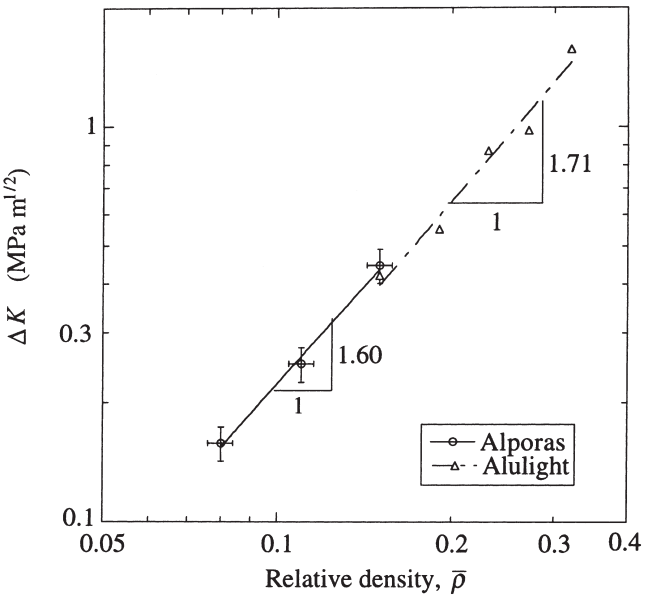

Fig. 6. Effect of relative density $\bar{\rho}$ on the stress intensity range ΔK required to give a crack growth rate da/dN=10^{-4} mm/cycle for Alulight and Alporas.

of the Al–Mg1–Si0.6 Alulight foam over a density range $0.15<\bar{\rho}<0.32$

$$\frac{da}{dN}=\left(\frac{da}{dN}\right)_0\left(\frac{\Delta K}{\bar{\rho}^{1.71}\Delta K_0}\right)^{20}, \quad (3)$$

and in like manner for Alporas over $0.08<\bar{\rho}<0.15$,

$$\frac{da}{dN}=\left(\frac{da}{dN}\right)_0\left(\frac{\Delta K}{\bar{\rho}^{1.60}\Delta K_0}\right)^{25}. \quad (4)$$

With the choice $(da/dN)_0=10^{-4}$ mm/cycle we have ΔK_0=10.5 MPa m$^{1/2}$ for Alulight, and ΔK_0=9.78 MPa m$^{1/2}$ for Alporas.

4.5. Effect of mean stress on the fatigue crack propagation response

Exploratory tests were conducted to examine the effect of mean stress (characterised by the load ratio, $R=P_{min}/P_{max}$) on the FCP response. The FCP rates from K-increasing tests at R=0.1, 0.3 and 0.5 are compared in Fig. 8 for Al–Mg1–Si0.6 Alulight and Alporas foams. It is noted that an increase in R value from 0.1 to 0.5 more than doubles the slope m of the crack resistance curves, and the effect of mean stress can be captured approximately by using $\sqrt{\Delta K K_{max}}$ as the combined loading parameter.

4.6. Effect of a single peak overload on the fatigue crack propagation response

In order to investigate the effect of a single peak overload on the FCP response, constant ΔK tests, interrupted

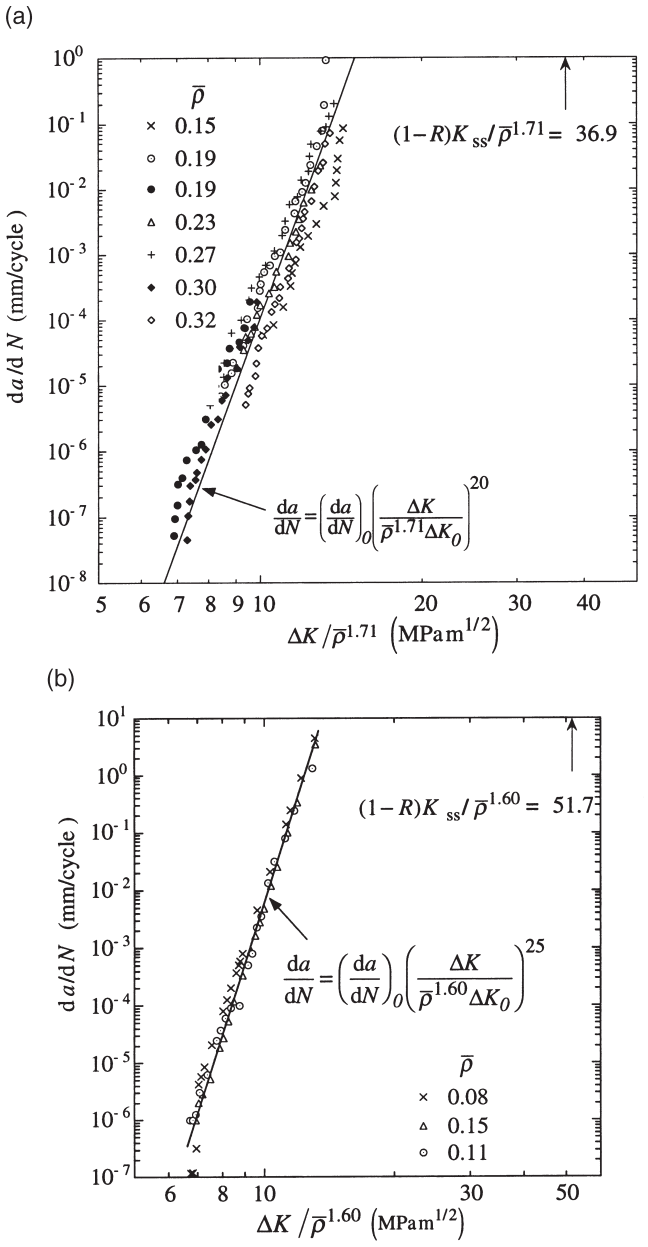

Fig. 7. (a) Effect of relative density on the da/dN versus $\Delta K/\bar{\rho}^{1.71}$ response of Alulight foam; taking $(da/dN)_0=10^{-4}$ mm/cycle gives ΔK_0=10.5 MPa m$^{1/2}$. (b) Effect of relative density on the da/dN versus $\Delta K/\bar{\rho}^{1.60}$ response of Alporas foam; taking $(da/dN)_0=10^{-4}$ mm/cycle gives ΔK_0=9.78 MPa m$^{1/2}$.

by a single peak overload, were performed on compact tension specimens of the Al–Mg1–Si0.6 Alulight and Alporas foams at R=0.1. Fig. 9(a) presents the results for two Alulight specimens ($\bar{\rho}$=0.30) which were tested at the baseline stress intensity ranges of ΔK=1.40 MPa m$^{1/2}$ and ΔK=1.32 MPa m$^{1/2}$, while Fig. 9(b) shows the case for Alporas ($\bar{\rho}$=0.08) tested at ΔK=0.12 MPa m$^{1/2}$.

In each case, the crack was grown at the baseline stress intensity range for several mm before overloads of range $\Delta K_{OL}=1.8\Delta K$ and $1.5\Delta K$ were applied to the Alulight and Alporas, respectively. The baseline loading

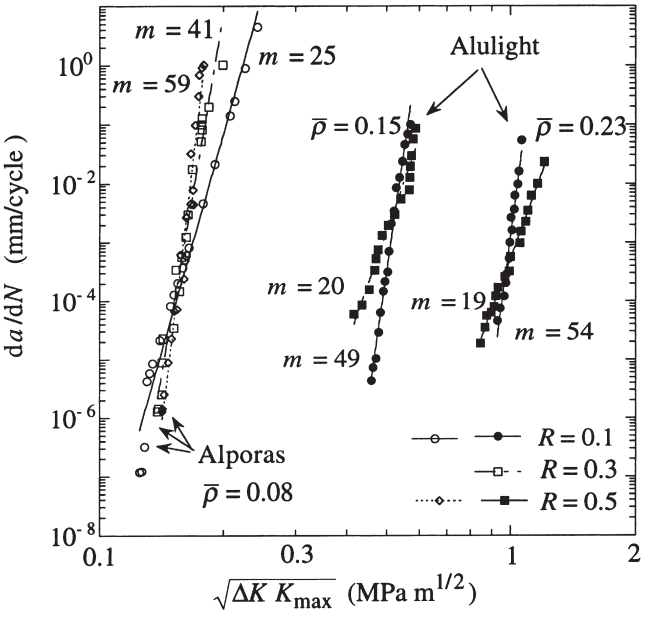

Fig. 8. Effect of load ratio R on the da/dN versus $\sqrt{\Delta K K_{max}}$ response. K-increasing tests on compact tension specimens of Alporas foam (open symbols) and Alulight foam, composition Al–Mg1–Si0.6 (full symbols).

was then resumed. Throughout, the crack length was measured using the DC potential drop method and gave the same crack length evolution as the back-face compliance technique and visual observation using a travelling microscope. In all cases, the single peak overload caused the crack to advance by 1–2 mm, but once baseline loading had been resumed the growth rate returned to its pre-overload value. To within the resolution of the crack extension measurements, neither crack retardation nor crack acceleration was evident. It was not possible to apply larger overloads due to the low toughness of the foams.

We recall that for fully dense metals, crack growth retardation occurs over a crack extension approximately equal to the overload plastic zone size, r_{OL}

$$r_{OL} \approx \frac{1}{\pi}\left(\frac{K_{OL}}{\sigma_{pl}}\right)^2, \tag{5}$$

where K_{OL} is the peak stress intensity factor at overload. On substituting values, we find that $r_{OL}\approx$70–80 mm for the Alulight and $r_{OL}\approx$5 mm for the Alporas specimens. Since the ligament width of the Alulight is about 25 mm, this implies that the overload produced net section yielding, invalidating the use of K as the loading parameter for the overload cycle. The tests remain useful, however, as an exploratory means of assessing load interaction effects under variable-amplitude loading. It is concluded that overloads do not induce crack growth retardation in these foams. This is not surprising, as we shall argue below that the crack advance mechanism is by fatigue failure of the cell edges behind the crack tip. In contrast,

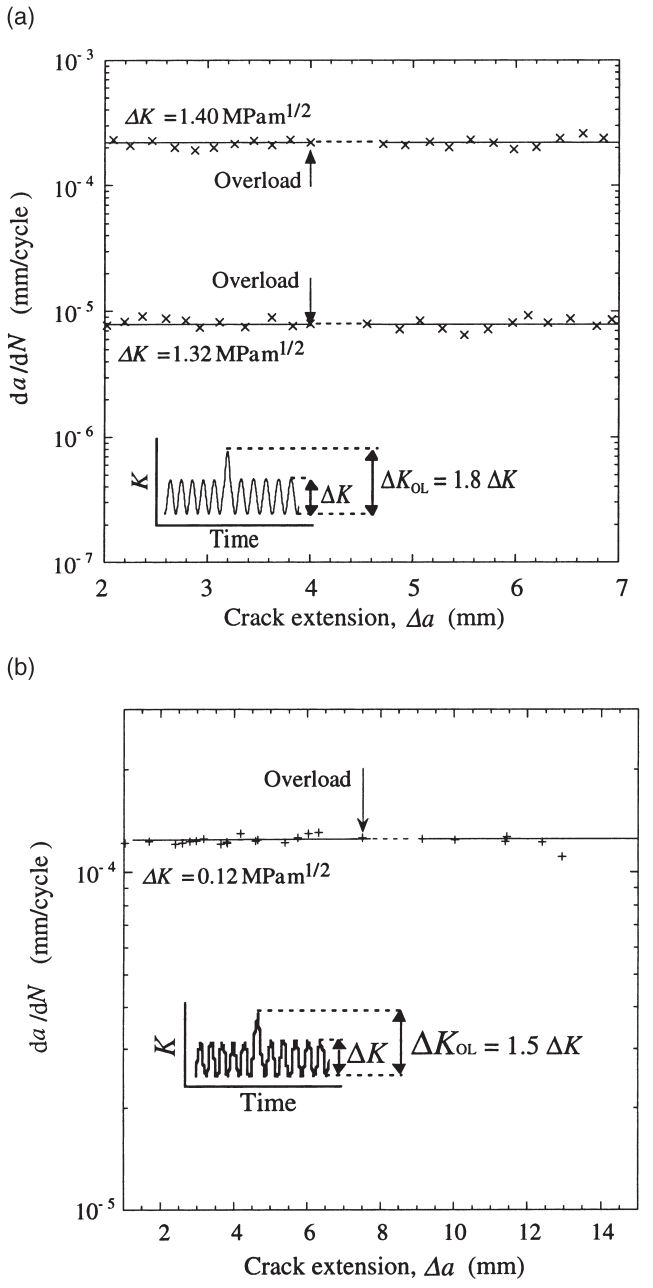

Fig. 9. Effect of a single peak overload on da/dN. K-constant tests at R=0.1 on compact tension specimens of (a) Alulight foam, composition Al–Mg1–Si0.6 with $\bar{\rho}$=0.30, and (b) Alporas foam, $\bar{\rho}$=0.08.

load interaction effects in fully dense alloys are due to premature crack closure as the crack advances into the overload plastic zone (see, for example, [16]).

5. The mechanism of fatigue crack propagation

Visual observations revealed that fatigue cracks grow approximately along the centreline of the Alulight and Alporas CT specimens, apparently following the weakest path from cell to cell. Away from the fracture plane, no cell edge cracking is evident. The main fatigue crack advances by the sequential failure of cell faces ahead of the tip. The cell edges behind the crack tip fail later, and the rate of fatigue failure of the cell edges behind the crack tip appears to control the overall rate of crack advance. It is recalled that the extent of crack bridging is limited to about one cell dimension, as shown in the side view of Alulight, Fig. 2. This interpretation is supported by the fact that the local crack growth rate is retarded when a thick cell edge is encountered and crack growth is most rapid through large cells.

The difference in crack bridging is striking for fatigue crack growth (bridging over a single cell) and monotonic loading (bridging zone of length about four cell sizes). It appears that fatigue failure severely degrades the degree of crack bridging compared to that observed in a fracture toughness test. This is supported by the fact that the observed ΔK levels in a fatigue crack growth test at high growth rates (da/dN≈1 mm/cycle) are significantly smaller than the steady-state fracture toughness values $(1-R)K_{ss}$, see Figs. 3 and 7. This phenomenon of reduced bridging under fatigue loading has been noted previously for the case of ceramic composites bridged by metallic fibres [17]; again, fatigue failure degrades the bridging strength behind an advancing crack tip.

Examination of the fracture surfaces in a scanning electron microscope reveals that the crack advanced by microvoid coalescence under both cyclic and monotonic loading, see Fig. 10.

6. Concluding remarks

The mode I fatigue crack propagation (FCP) responses of the closed-cell aluminium-based foams Alulight [compositions Al–Mg1–Si0.6 and Al–Mg1–Si10 (wt%)] and Alporas have been measured for a relative density in the range 0.1 to 0.4. Linear elastic fracture mechanics can be used to characterise fatigue crack advance. The classic sigmoidal variation of log da/dN with log ΔK is evident, with a Paris-law exponent m≈20–25. The high sensitivity of da/dN to ΔK suggests that a conventional damage-tolerant approach is impractical for design purposes; instead, it is recommended that design is based on keeping the applied stress intensity range below the FCP threshold ΔK_{th}.

For a given value of crack growth rate, the resistance ΔK scales with $\bar{\rho}^{1.71}$ for Alulight and with $\bar{\rho}^{1.60}$ for Alporas. Increasing the mean applied stress increases the Paris-law exponent and, for a given ΔK, increases the crack growth rate da/dN. If the applied fatigue loading is characterised by $\sqrt{\Delta K K_{max}}$, the results for crack growth rate from the R=0.1 and R=0.5 tests intersect at da/dN≈10^{-3} mm/cycle. A preliminary study has been made of load interaction effects: the injection of a single

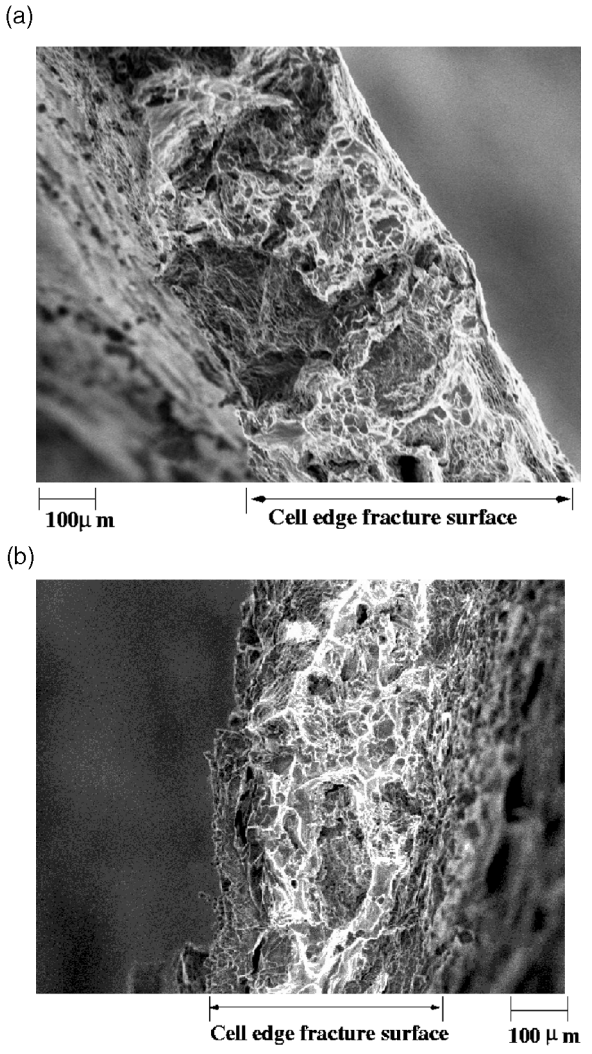

Fig. 10. Comparison of scanning electron micrographs of the fracture surfaces from cyclic and monotonic crack growth tests. Compact tension specimens of Alporas foam, $\bar{\rho}$=0.11. (a) Fatigue crack propagation test (*K*-increasing, *R*=0.1) and (b) fracture toughness test.

peak overload into constant baseline loading gives rise to neither crack growth acceleration nor retardation.

Acknowledgements

The authors are grateful to the EPSRC for financial support. Additional funding came from DARPA/ONR through MURI grant number N00014-1-96-1028 on the Ultralight Metal Structures project at Harvard University. The authors also wish to thank Dr F. Simancik of Mepura for supplying the Alulight foams, Dr T.J. Lu and Dr J.E. Huber for constructive comments, and A. Heaver and S. Marshall for their technical assistance.

References

[1] Baumeister J, Schrader J. Methods for manufacturing foamable metal bodies. German Patent DE 41 01 630, 1991.
[2] Davies GJ, Zhen S. Metallic foams: their production, properties and applications. J Mater Sci 1983;18:1899–911.
[3] Akiyama S, Imagawa K, Kitahara A, Nagata S, Morimoto K, Nishikawa T, et al. Foamed metal and method of producing the same. US Patent 4,713,277, 1987.
[4] Sang H. Process for producing shaped slabs of particle stabilized foamed metal. US Patent 5,334,236, 1994.
[5] Banhart J, editor. Proceedings of Metallschaume Conference on Metal Foams, Bremen, Germany, 6–7 March 1997. Bremen: MIT Publications, 1997.
[6] Ashby MF, Evans AG, Hutchinson JW, Fleck NA. Metal foams: a design guide. Oxford: Butterworth Heinemann, 2000.
[7] Olurin OB, Fleck NA, Ashby MF. Fatigue of an aluminium alloy foam. In: Proceedings of IFAM Conference on Metal Foams and Porous Metal Structures, Bremen, Germany, 16–16 June 1999. Bremen: MIT Publications, 1999.
[8] McCullough KYG, Fleck NA, Ashby MF. The stress–life behaviour of aluminium alloy foams. Fatigue Fract Eng Mater Struct 2000;23:199–208.
[9] McCullough KYG, Fleck NA, Ashby MF. Uniaxial stress–strain behaviour of aluminium alloy foams. Acta Mater 1999;47(8):2323–30.
[10] McCullough KYG, Fleck NA, Ashby MF. Toughness of aluminium alloy foams. Acta Mater 1999;47(8):2331–44.
[11] ASTM E647-95, Standard test method for measurement of fatigue crack growth rates. Philadelphia (PA): American Society for Testing and Materials, 1995.
[12] Fleck NA. An investigation of fatigue crack closure. In: Ph.D. thesis. Cambridge: Cambridge University, 1984.
[13] Richards CE, Deans WF. In: The measurement of crack length and load using strain gauges. Birmingham, UK: EMAS Publications, 1980:28.
[14] Olurin OB, Fleck NA, Ashby MF. Deformation and fracture of aluminium foams. Mater Sci Eng A 2000;A291:136–46.
[15] Suresh S. Fatigue of materials. Cambridge: Cambridge University Press, 1991.
[16] Fleck NA. Influence of stress state of crack growth retardation. In: Fong JT, Fields RJ, editors. Basic questions in fatigue. Philadelphia (PA): American Society for Testing and Materials, 1984:157–83.
[17] Akisanya AR, Fleck NA. Fatigue and creep of a constrained metal wire. Acta Metall Mater 1993;41(1):121–31.